Metal Decorated Multi-Walled Carbon Nanotube/Polyimide Composites with High Dielectric Constants and Low Loss Factors

S. Ghose[1], K.A. Watson[1], H.A. Elliott[2], K.J. Sun[2], K.L. Dudley[2], J.G. Smith, Jr. [2], and J.W. Connell[2]
[1]National Institute of Aerospace, 100 Exploration Way, Hampton, VA 23666, USA
[2]NASA Langley Research Center, MS 226, Hampton, VA 23681, USA

Corresponding author: Kent A. Watson, kent.a.watson@nasa.gov, 1-757-864-4287

SUMMARY

Nanocomposite materials comprised of metal decorated multi-walled carbon nanotubes were prepared and characterized. Electromagnetic characterization showed that certain sample configurations exhibited a decoupling of the permittivity (ε') and loss factor (ε") indicating that these properties could be tailored within certain limits.

Keywords: Dielectric materials, carbon nanotubes, permittivity, loss factor

INTRODUCTION

Tunable and tailorable dielectric materials are critical technologies necessary to meet and advance science and engineering goals important in many commercial, industry, and government technology development programs. Unfortunately tailorable materials to date have been limited in bandwidth and suffer unacceptably high losses.

An ideal semiconducting material should have a relatively high electrical permittivity, good thermodynamic stability, and a high interface quality. Of these characteristics, electrical permittivity is important in the design of electronic components and describes the manner in which a particular dielectric material affects an incident electric field [1]. The electrical permittivity of a given dielectric material is often expressed via the dielectric's complex electrical permittivity (ε), a term containing both an energy storage term (ε') which is ideally maximized, and an electrical loss term (ε"), i.e., the loss factor, that is ideally minimized. Likewise, the electrical losses can be expressed as the tangent of the dielectric loss angle (δ), i.e., the loss tangent. A material's loss factor (ε") is the product of its loss tangent and known dielectric constant (ε_r), and therefore the ε" and the loss tangent (tan δ) are interrelated characteristics. An ideal dielectric would therefore have a relatively high ε' value accompanied by a minimal ε". However, in most naturally-occurring dielectrics a relatively high ε' typically coincides with relatively high ε", which can potentially render an otherwise satisfactory dielectric less than optimal when it is used for certain purposes or applications.

Our group has developed a simple method for the decoration of multi-walled carbon nanotubes (MWCNTs) with metal nanoparticles [2, 3]. The process involves dry mixing of metal salt (e.g. a metal acetate) with MWCNTs followed by heating in an inert

atmosphere. The procedure is scalable and applicable to various carbon substrates (e.g. graphite, etc.) and many metal salts (e.g. Ag, Au, Co, Ni, Pt and Pd acetates).

The characterization of metal decorated MWCNTs has led to a significant breakthrough in the area of tailorable dielectric materials. It was noted that with the preferential alignment of Ag-decorated MWCNTs in a polymer matrix, a decoupling of ε' in relation to ε" and tan δ occurred [4]. The disconnection between the dielectric and the loss factor were found to be controlled by varying the wt% of Ag particles decorating the MWCNTs. The decoupling of these electrical parameters offers a class of materials useful in a variety of applications in electronics and electromagnetics with potential applications into the optical frequency regime [5-7]. Other applications include low-mass ultra-thin microstrip antennas, fuel cell components, and as potential materials for High-K gate dielectrics in Complementary Metal-Oxide-Semiconductor (CMOS) technology [8].

EXPERIMENTAL

Ag/MWCNT Synthesis and Characterization

The procedure for preparing Ag-decorated MWCNTs involves heating a mixture of MWCNTs and Ag salt under nitrogen for 3-5 hours [22]. Three samples (Table 1) were prepared – the first where the theoretical amount of metallic Ag was 9% by weight, the second where it was 23% by weight and the third where it was 33% by weight. High resolution scanning electron microscopy (HRSEM) images were obtained using a Hitachi S-5200 field emission scanning electron microscope equipped with an Energy Dispersive Spectroscopy (EDS) detector (EDAX). X-ray diffraction (XRD) analyses were performed on a Siemens D5000 X-ray diffractometer with Cu K_α as the radiation sources ($\lambda = 1.5418$ Å).

Materials Processing

To determine the effect of Ag/MWCNT alignments on the electromagnetic properties, Ag/MWCNT/polymer samples were prepared as described below.

Table 1. Ag/MWCNT Samples

Sample	Sample details
Ag-1	9 wt% Ag attached to MWCNTs; 20 wt% of the mixture added to Ultem™. Polymer matrix: filler = 18.2 wt% MWCNT and 1.8 wt% Ag.
Ag-2	23 wt% Ag attached to MWCNTs; 20 wt% of the mixture added to Ultem™. Polymer matrix: filler = 15.4 wt% MWCNT and 4.6 wt% Ag.
Ag-3	33 wt% Ag attached to MWCNTs; 20 wt% of the mixture added to Ultem™. Polymer matrix: filler = 13.3 wt% MWCNT and 6.7 wt% Ag.

Parallel Alignment to Flow Direction

The MWCNT/Ag samples were melt-mixed at a loading level of 20 wt% with Ultem™ 1000 (GE Plastics) in a Brabender Plasticorder PL 2000 (30 cc capacity) at a temperature of 325 °C and 25 rpm for 3 hours. After mixing, the material was ground in a Mini-Granulator and then extruded through a Laboratory Mixing Extruder at a barrel temperature of 170 °C and a die (0.38 mm x 19.1 mm) temperature of 350 °C. The primary purpose of extrusion was to align the MWCNTs in the direction of flow.

Perpendicular Alignment to flow direction

Once extruded, the ribbons were cut into pieces (about 2 cm x 2 cm), stacked on one side of a 9 cm x 2 cm x 3 cm (i.d.) mold and the remainder of the mold filled with Ultem™ 1000 pellets. The stacked ribbons were compression molded at 270 °C, 1.72 MPa, for 3 hours. The samples were then sliced using an Isomet low speed saw.

Electromagnetic Characterization

A HP 8510C Vector Network Analyzer (VNA) was used to measure the scattering parameters of the baseline polymer material matrix and the aligned MWCNTs. Energy from the VNA was generated by an RF source and directed from the test port through an X-band (8.2-12.4 GHz) waveguide and into target materials. The dielectric properties were calculated using a data acquisition computer and the HP 85071E Materials Measurement software. The various material parameters such as the real and imaginary parts of permittivity and the loss tangent were plotted as a function of frequency. Prior to conducting material measurements, a "Full 2-Port" VNA calibration was performed. The calibration corrects for systematic measurement errors inherent to the instrument by referencing known boundary conditions [9].

Sample Preparation for Electronics Characterization

The MWCNT/Ag polymer ribbon samples were cut and stacked to fit a waveguide sample holder corresponding to the test frequency band of interest. An optical breadboard test fixture and positioner with mounted waveguide apparatus were used.

Electrical and Magnetoresistance Measurements

Electrical resistance measurements were conducted on extruded samples of Ultem™/MWCNT/Ag composites as a function of temperature at a zero magnetic field, and as a function of magnetic field at constant temperatures. Four electrical leads were attached onto the sample surface using Ag paint. Separation of the neighboring electrodes was 1-2 mm, and the length of the electrodes was 5-6 mm. The studied sample was placed in the cryostat where the temperature of the sample could be varied and a magnetic field (H) could be applied in parallel to the sample surface. For the magnetoresistance measurement, the sample temperature was set at a pre-determined value while magnetic field scanned from 5 to -5. Magnetoresistance was calculated using R(H)/R(0) - 1, where R(0) was the electrical resistance at zero magnetic field and H was the magnetic field strength. Results of the resistance measurements include those where voltages were applied parallel and perpendicular to the axial direction of MWCNTs. Curves of surface resistivity of the conducting samples as a function of temperature for both directions of the applied voltages were plotted. I-V curves (current vs. voltage) were obtained by measuring the current as voltage was scanned from negative to positive values. Differential resistance/conductance can thus be calculated and plotted against applied voltage.

RESULTS AND DISCUSSION

Sample Characterization

The HRSEM image of Ag-1 (Figure 1, left) shows Ag particles between 40 and 60 nm in size attached to the MWCNTs. Metallic silver was confirmed by EDS (Figure 1, right) which indicated the presence of Ag particles on the MWCNTs. The Fe peak was from the catalyst in the MWCNTs and the Al and Au peaks were from the stub and the paste, respectively. As shown in Figure 2, the XRD spectrum of both Ag-1 and Ag-2 exhibited the signature peaks of zero-valence Ag metal at 38.0°, 44.2°, 64.3°, and 77.2°, corresponding to the (111), (200), (220), and (311) crystal planes of Ag^0, respectively. The lack of acetate diffraction patterns suggested that the conversion to Ag metal was essentially complete.

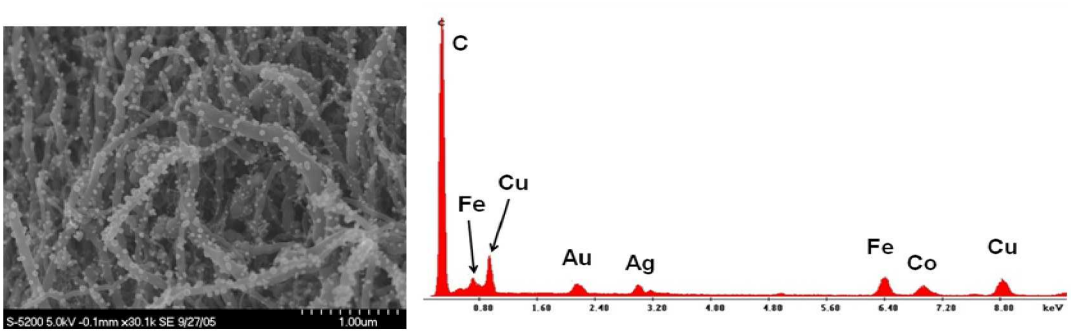

Figure 1: HRSEM of Ag-1 (left), EDAX on sample (right)

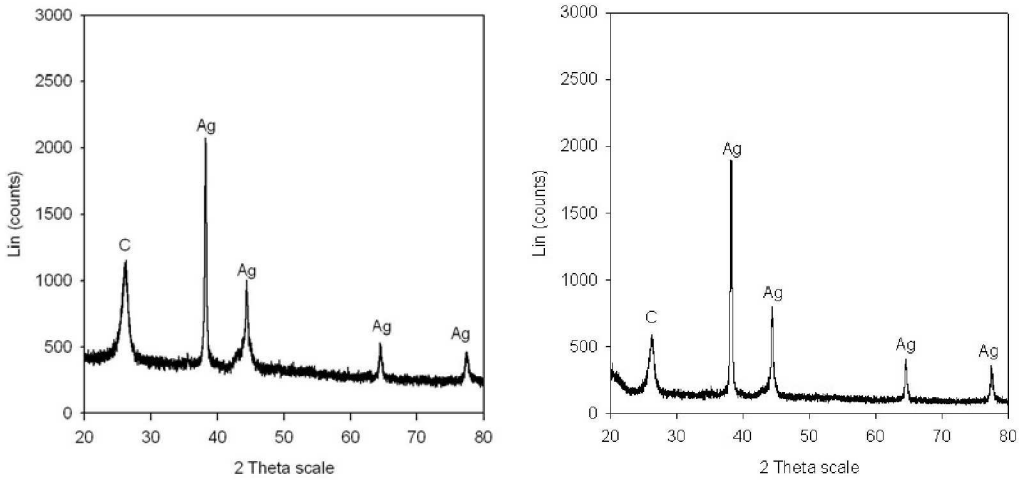

Figure 2: XRD patterns of MWCNT/Ag mixtures of Ag-1 (left) and Ag-2 (right).

Figure 3 shows the HRSEM images of the Ag/MWCNTs after melt mixing with Ultem™ and extrusion of the mixture. The MWCNTs were predominantly oriented in the direction of extrusion (denoted by the arrow).

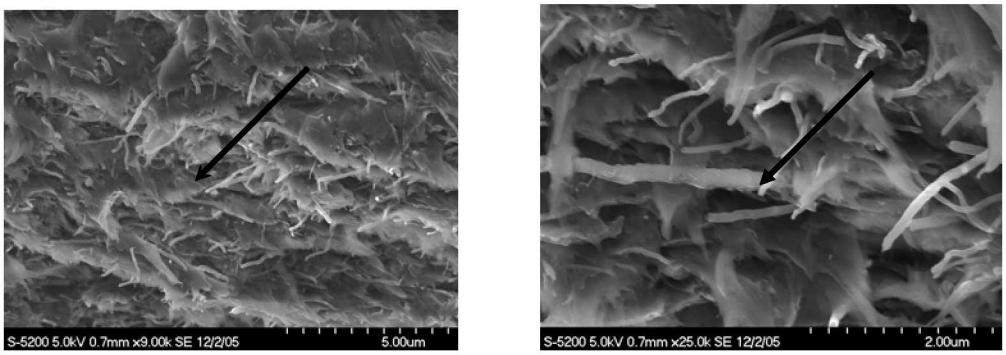

Figure 3: HRSEM of Ag-1; arrows denotes flow direction

Electrical Resistance

Electrical resistivities of the samples were found to vary with Ag%. The 20 wt% MWCNT (without Ag) samples had the lowest resistivity. At room temperature, it was 70 -200 ohm/mm^2 depending on applied voltage orientation. Higher resistance was observed when the applied voltage was perpendicular to the MWCNT alignment.

The resistivity of the Ag-1 samples was 250-350 ohm/mm^2 while that of the Ag-3 samples was 1x10^5 ohm/mm^2. With 20 dc Volts applied, the Ag-2 samples were categorized as insulators with unstable currents in the pico-ampere range. Figure 4 exhibits the surface resistivity curves of the conducting samples as a function of temperature for both directions of the applied voltages. As observed, the resistance had a relatively pronounced increase at low temperatures for all samples. The increases were slightly larger when voltages were applied in the parallel direction. The Ag-1 samples have higher resistance than the 20 wt% MWCNT composites and was most likely due to the lower loading of MWCNTs in the Ag/MWCNT-Ultem™ mixture. The 9 wt% Ag was not sufficient for compensating the loss of current conduction because of a lesser amount of CNTs, however, it seemed to improve the conduction between CNTs, as was revealed by the decrease in anisotropy of resistivity. Furthermore, resistance data of the 20 wt% MWCNT and Ag-1 samples could be fitted with the curves of Exp(C/T) (where C is a MWCNT loading dependent constant) from room temperature to 5 K, and that of the Ag-3 samples from 200 K to 5 K. The exponential proportion to 1/T could be an indication of currents being conducted via a tunneling mechanism. Figure 5 shows the temperature dependent variations of currents for the same set of samples where the currents were normalized to their respective magnitude at 100 K. It could be observed that, instead of increasing with temperature as those of 20% MWCNT and Ag-1 samples, currents in Ag-3 samples decreased with increasing temperature at temperatures above 200 K, for both orientations of the applied voltages. The decrease in current with increasing temperature was a metal-like behavior and implied that, at high temperatures, a substantial portion of currents were conducted through the Ag components in the composites. This was also indicated by the data of differential conductance. However, at low temperatures, conduction through CNTs and tunneling through the contacts of CNTs were the predominant mechanisms for transporting the electrons.

Regarding the insulation of Ag-2, it may be that the 23 wt% of Ag had a large enough mass to enhance potential barriers for preventing electrons from tunneling between

CNTs, but it was under the threshold for electrons to find a conduction network for percolating.

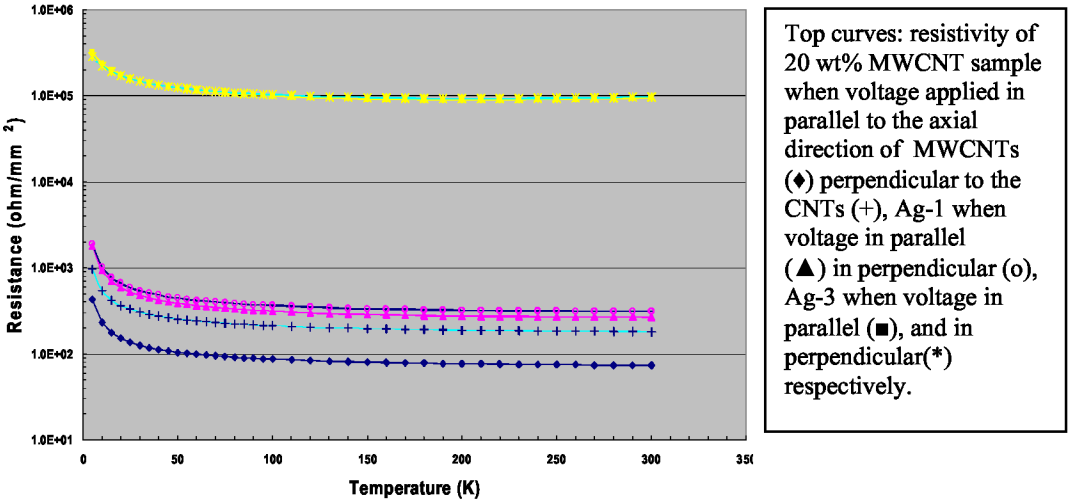

Figure 4: Temperature dependent electrical resistivity of MWCNTs-loaded Ultem™ composites.

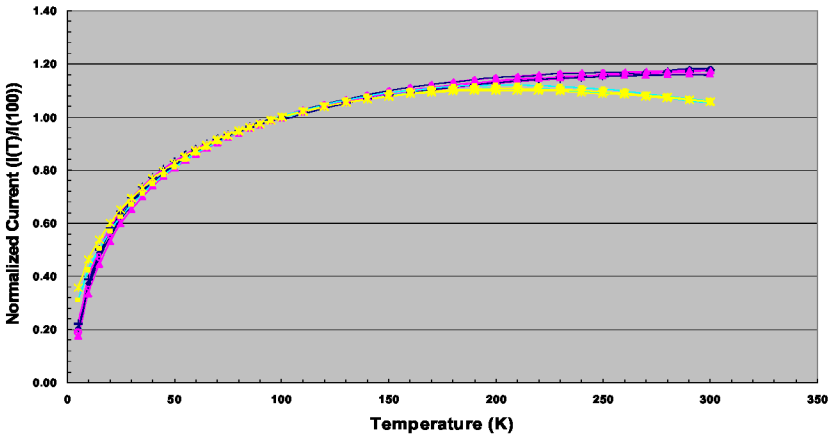

Figure 5: Normalized currents as a function of temperature for the samples of 20 wt% MWCNT (curves with ♦ and +), Ag-1 (▲ and O), and Ag-3 (■ and *) composites.

Magnetoresistance

Figure 6 displays the magnetoresistance as a function of magnetic field at temperatures of 3, 5, 10, 20, 50, 100, and 200 K for the Ultem™/20% MWCNTs composite samples. Voltage was applied in the direction perpendicular to the axial direction of the MWCNTs. The magnetoresistance of the composite was negative and decreased monotonically with the increasing magnitude of magnetic field. Also, the magnetoresistance was enhanced in magnitude at low temperatures. No magnetic hysteresis was observed. Figure 6 exhibits the typical magnetoresistance behavior of composites. The loading level of Ag affected the magnetoresistance quantitatively. For samples with the same loading, the voltage applied in the perpendicular direction had a larger response to the applied magnetic field as compared to the parallel direction.

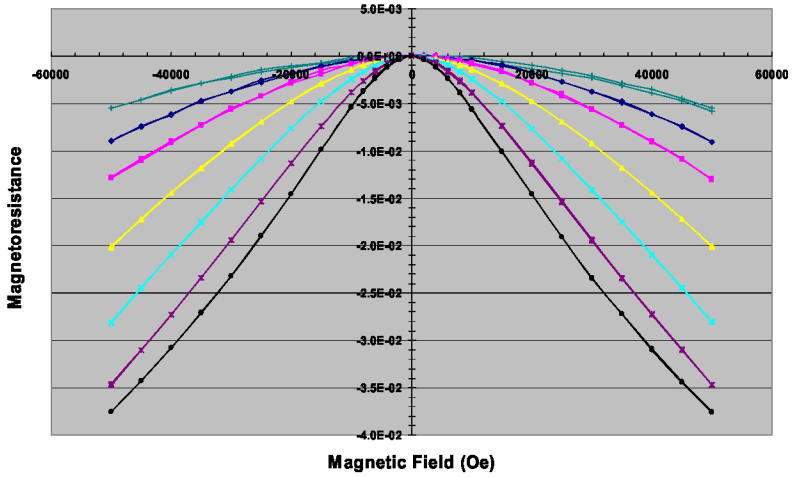

Figure 6: Magnetoresistance at various temperatures for 20 wt% MWCNT-Ultem™. From bottom to top: magnetoresistance at 3, 5, 10, 20, 50, 100, and 200 K.

I-V curves were obtained by measuring the current when the voltage was scanned from negative to positive values. For 20 wt% MWCNT and Ag-1 composites, differential conductance increased with voltages at temperatures lower than 100 K and remained constant at temperatures ≥100 K. For the Ag-3 composites, the differential conductance increased with voltages at all temperatures and showed slope changes at higher voltages. Figure 7 compares the normalized differential conductance of the Ag-1 samples when voltage was applied in parallel to the MWCNTs at a temperature of 3 K with those when the voltage applied was in the perpendicular direction. The differential conductance (dI/dV) was normalized to its value at 0 voltages. A dip on the curve at low voltages (|V|< 0.2V) was considered as a suppression of conductance and was even more pronounced for the perpendicular direction. The dip was attributed to the strong electron-electron (e-e) interaction in and between the MWCNTs. With the strong e-e interaction, a coulomb gap may be opened and electron motion was via the hopping mechanism. These dips did not show up at high temperature. The suppression of conductance was also observed for the 20 wt% MWCNT composites.

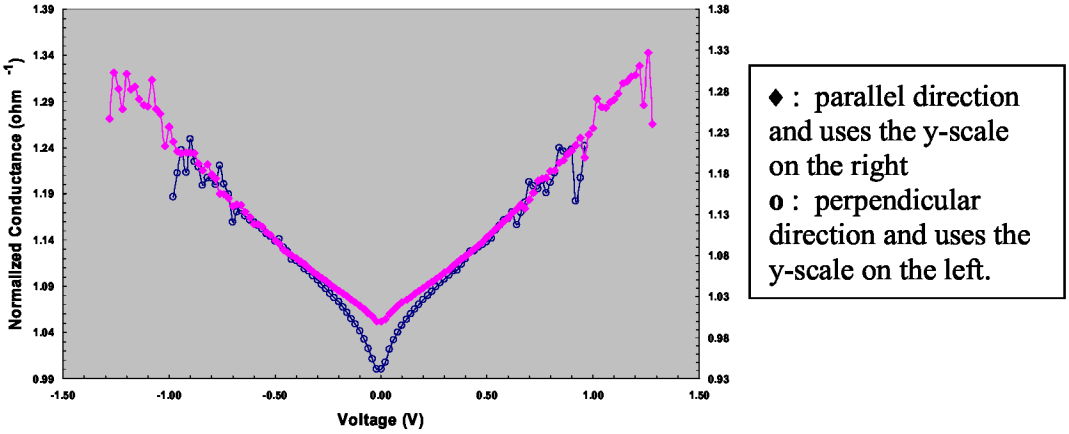

Figure 7: Comparison of normalized differential conductance of Ag-1 samples for both directions of the applied voltage at 3K.

Electromagnetic Properties

The materials used for testing were comprised of extruded samples of MWCNTs, decorated with and without Ag particles, dispersed in an Ultem 1000™ matrix and have a preferential alignment (horizontal, vertical or longitudinal) with respect to an orientation of an electrical field that was incident to the length-wise axis of the tubes.

In the horizontal alignment, [Figure 8(a)], the CNTs were aligned with respect to the orientation of the electrical field (arrow E). Incidental energy (propagating in the direction k) entered the dielectric through the first port (Port 1), with some portion of the incident energy (flowing in the direction k) being reflected as represented by the arrow R. Transmitted energy (arrow T) exited the dielectric through a second port (Port 2). Energy was also attenuated (A not shown) within the material, thus reducing the magnitude and altering the phase of the transmitted energy. By means of a law of conservation the reflected energy (R) + (T) + (A) must equal the total energy. From this conservation relationship the loss within the dielectric was determined [10, 11]. Data was obtained at 10 GHz. Figure 8(b) shows that the magnitude of the energy storage term (ε') was at a minimum for the neat polymer. As the MWCNT loading level was increased, the magnitude of ε' increased significantly. However, this potentially desirable increase in ε' came with a tradeoff in the form of higher losses in the dielectric. When samples containing 20% Ag were tested, the magnitude of ε' was clearly reduced by the presence of the Ag nanoparticles. However, for the Ag-1 samples, the magnitude of ε' remained relatively high compared to the 0, 5, and 10 wt% samples. For Ag-2 samples, the magnitude of ε' was approximately equal to that of the 5 wt% MWCNTs. A similar pattern was observed in case of the loss factor (ε") that was clearly reduced by the introduction of the Ag nanoparticles. In Ag-1, ε" was reduced by approximately 75%, with an approximate 30% reduction in the magnitude of the ε'. For Ag-2 ε" was effectively reduced to zero. Therefore, by varying the Ag loading % of the Ag, the loss factor was minimized without minimizing the value of ε'. The magnitude of tan δ was plotted against the material loading % and the values increased sharply when the loading level of MWCNTs was increased from 10 to 20 wt%. Upon addition of Ag into a horizontally-aligned network, the magnitude of tan δ was reduced by approximately 70% in Ag-1 samples. For Ag-2, tan δ was effectively reduced to zero.

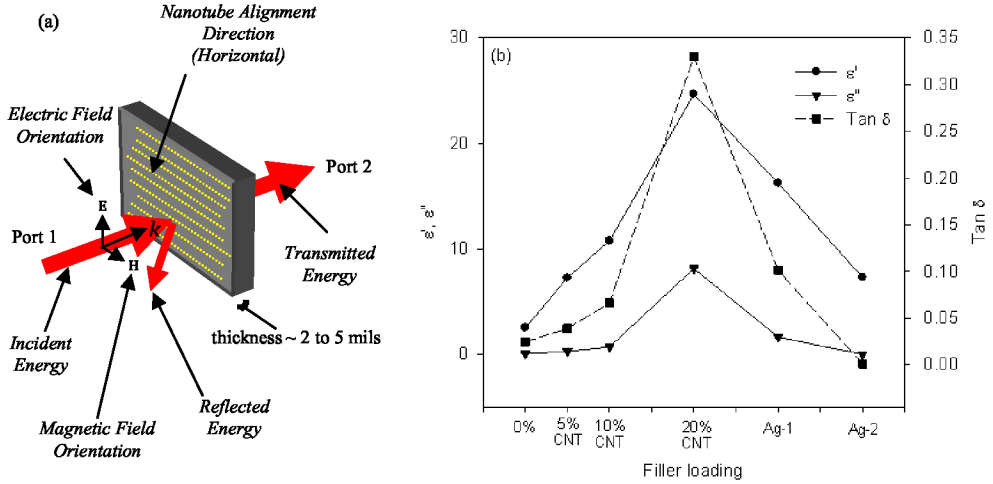

Figure 8: Permittivity, loss, and loss tangent of horizontally aligned samples

Figure 9(a) denotes an experimental set-up with the orientation of the MWCNT network being vertical to the applied field. Figure 9(b) shows that the magnitude of ε' increased dramatically as the MWCNT loading percentage increased from 10 to 20 wt%. For Ag-1, this magnitude decreased slightly but remained higher than that exhibited during horizontal alignment. Additional loading of Ag (Ag-2) had a negligible effect on the magnitude of the energy storage value. When the MWCNT loading increased from 10 to 20%, ε" likewise increased. However, ε" was substantially reduced with the introduction of Ag in Ag-1. Figure 10(b) also shows an approximate 90% reduction in ε" which corresponded to a lower reduction in the magnitude of the ε'. Likewise, an approximately 90% reduction in the loss tangent was observed between a peak value at 20 wt% MWCNT loading and Ag-1. Additional Ag loading had a negligible effect on ε" and tan δ.

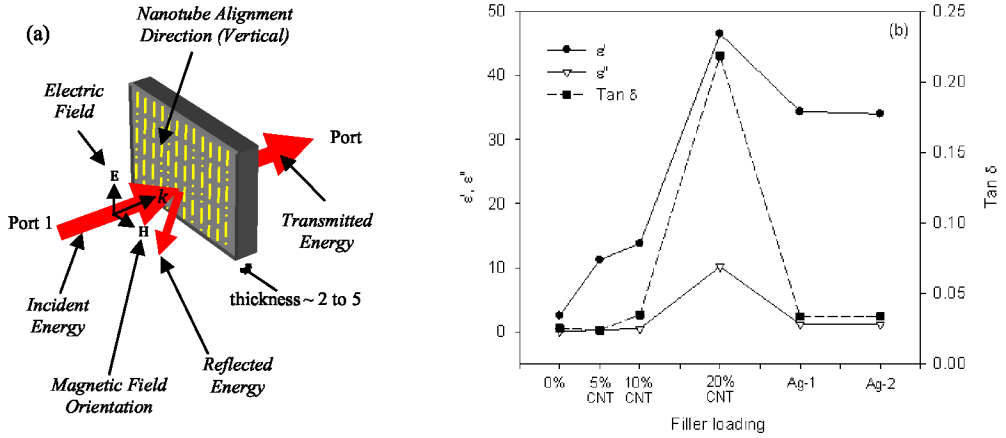

Figure 9: Permittivity, loss, and loss tangent of vertically aligned samples

Based on the data shown in Figures 8 and 9, it can be concluded that the MWCNT/Ag samples demonstrate a unique ability to "decouple" the energy storage term of a given material's electrical permittivity from the materials' electrical loss term when oriented in a preferential manner. The ε' and ε" of these materials could be effectively decoupled from each other and independently controlled by varying the alignment of the network, the wt% of the metal particles, or the size of the particles.

SUMMARY

Ag-decorated MWCNTS were prepared and then compounded with a polyimide and extruded to preferentially align the MWCNTs. Extruded samples were examined by a variety of electromagnetic experiments. Electrical resistivity of the samples was found to vary with the percentage of Ag. It was observed that the currents increased with temperature in the MWCNT loaded composites as well as the Ag-1 composites. However, currents in the samples of Ag-3 composites decreased with increasing temperature at temperatures above 200 K, for both orientations of the applied voltages. The decrease in current with increasing temperature was a metal-like behavior and implied that, at high temperatures, substantial portion of currents were conducted through the Ag components in the composites. The data also showed differential conductance at low temperatures indicating that the conduction was through the CNTs via contacts and a tunneling mechanisms. Similarly, at low voltages, the currents were

mainly conducting through the MWCNTs, as those in the samples of 20 wt% MWCNTs and Ag-1 composites whereas, at higher voltages, the currents had more conducting paths through the silver.

For electromagnetic properties, the network of MWCNTs (with or without Ag) was preferentially aligned with respect to an incident electrical field. For Ag-1 and Ag-2 samples aligned horizontally, ε' was effectively decoupled from ε". This decoupling effect of the energy storage value from the electrical loss value was tailorable by varying the preferred alignment of the network and/or the loading percentage of the nanoparticles, and/or by varying the size and/or distribution of the metal-based nanoparticles. This opens up a pathway to generate a class of engineered dielectric materials that could be useful in a host of applications such as a potential material for use in Complementary Metal-Oxide-Semiconductor (CMOS) technology, microwave engineering applications, RF communications and controls and optics.

ACKNOWLEDGEMENTS

The authors wish to acknowledge the help received from Dennis C. Working of NASA LaRC and Dr. Peter T. Lillehei of NASA LaRC for his valuable comments.

REFERENCES

1. A. R. Von Hipple, "Dielectrics and Waves", John-Wiley, 1954.

2. United States Patent Application No. 20070292699, December 20th 2007. WIPO Pub No.: WO/2008/048349, Pub date April 24th 2008.

3. Y. Lin, et. al, ACS Nano available online March 2009.

4. United States Patent Application No. 20090022977, January 22, 2009.

5. C.P. Poole Jr. et. al., John Wiley and Sons, Inc. Hoboken, New Jersey, 2003.

6. D.A. Genov, et. al., Nano Letters, 2004, Vol. 4 (1), 153.

7. I.R. Gbitov, et. al., J. Opt. Soc. Am. B, 2006, Vol. 23 (3), 535.

8. B.G. Streetman and S.Banerjee, "Solid State Electronic Devices", Prentice Hall, Upper Saddle River, New Jersey, 2000.

9. J. Baker-Jarvis, et. al., IEEE Transactions on Microwave Theory and Techniques, August 1990, Vol 38, 1096.

10. Y.L. Yang, et. al., Journal of Nanoscience & Nanotechnology, 2005, 5(6), 927.

11. Y.L. Yang, et. al., Advanced Materials, 2005, 17(16), 1999.